Journal of Orthopaedic Surgery and Research

RESEARCH

Open Access

# Synergistic influences of BMP9 and NGF on the osteogenic differentiation of C3H10T1/2 mesenchymal stem cells

Junyu Liu[1], Kun Yang[2], Gang Li[3] and Yinghui Tan[4*]

## Abstract

**Background** Bone morphogenetic protein 9 (BMP9) and nerve growth factor (NGF) are critical factors influencing osteogenic differentiation in mesenchymal stem cells (MSCs). While BMP9 has been recognized for its potent osteogenic capabilities, NGF's role in bone tissue engineering is less understood. This investigation delineated the synergistic link of BMP9 with NGF in driving osteogenic differentiation in C3H10T1/2 MSCs.

**Objective** To evaluate the combined impact of BMP9 and NGF on osteogenic markers' expression levels and the formation of calcified nodules in C3H10T1/2 cells, providing a basis for the enhanced bone regeneration strategies in tissue engineering.

**Methods** C3H10T1/2 cells were subjected to treatment regimens incorporating NGF at variable concentrations (10, 50, and 100 ng/ml) and BMP9, either as monotherapies or in combination. Osteogenic differentiation' comprehensive assessment was undertaken by quantifying early-stage markers (Runx2, Col I) and late-stage markers (OPN) via RT-PCR, Western blotting, ALP staining, and Alizarin Red S staining for mineralized matrix deposition.

**Results** NGF elicited a concentration-dependent augmentation of early osteogenic markers, with the 10 ng/ml dosage demonstrating maximal efficacy. BMP9 independently facilitated robust osteogenic differentiation, whereas the combinatorial treatment with BMP9 and NGF synergistically amplified the expression levels of Runx2, Col I, and OPN. Notably, this combined treatment yielded a remarkable enhancement in the deposition of mineralized extracellular matrix, as evidenced by a notable escalation in the size and density of calcified nodules relative to monotherapies.

**Conclusion** The findings unveiled the remarkable synergistic link of BMP9 with NGF in potentiating osteogenic differentiation in C3H10T1/2 MSCs. This dual-factor approach presents a compelling paradigm for advancing bone regeneration strategies, providing substantial promise for utilization in bone tissue engineering plus regenerative medicine.

**Keywords** Mesenchymal stem cells, BMP9, NGF, Osteogenic differentiation, Tissue engineering

*Correspondence:
Yinghui Tan
tanyhxqkq@163.com

Full list of author information is available at the end of the article

## Introduction

Fractures and bone defects represent prevalent clinical challenges, frequently addressed through grafting techniques utilizing autologous, allogeneic, or xenogeneic sources [1]. However, these conventional approaches are not without remarkable drawbacks, involving donor site morbidity, potential disease transmission, and difficulties in achieving seamless graft integration. Such limitations reflect the necessity for innovative and alternative strategies particularly for bone repair and regeneration [2, 3].

Tissue engineering represents a cutting-edge solution to the remarkable challenges associated with replicating bone tissue, striving to reconstruct structures that intricately emulate the architecture and functionality of native bone [4]. Mesenchymal stem cells (MSCs) are at the forefront of this paradigm, distinguished by their remarkable proliferative potential and their pluripotent capacity to differentiate into a spectrum of cell lineages, including osteoblasts, when exposed to microenvironmental stimuli [5]. The integration of MSCs into tissue engineering strategies, particularly for the restoration of complex fractures and structural defects arising from maxillofacial trauma, has yielded compelling outcomes. Advanced studies uncover the efficacy of MSCs in expediting osteogenesis, remarkably accelerating the deposition of new bone matrix, as well as markedly diminishing the temporal framework required for the integration and healing of autologous bone grafts [3, 6].

However, the inherent biological capabilities of MSCs, while promising, are frequently inadequate to achieve the robust bone regeneration required for clinical success [7]. Consequently, the strategic integration of osteogenic growth factors has become an indispensable pathway for enhancing MSC functionality. Among these factors, bone morphogenetic proteins (BMPs) have markedly garnered attention, with BMP9, also known as growth differentiation factor 2 (GDF-2), emerging as a pivotal agent in the transforming growth factor-β (TGF-β) superfamily [6, 8]. Distinguished by its exceptional osteogenic potency, BMP9 has demonstrated a superior capacity to induce bone formation relative to clinically approved BMP2 and BMP7. However, despite its demonstrated efficacy, the precise molecular pathways through which BMP9 modulates osteoinductive processes remain only partially delineated, reflecting the necessity of further mechanistic exploration to fully unveil its therapeutic potential [5, 6].

Nerve fibers, in conjunction with osteogenic growth factors, are essential to the intricate process of bone regeneration. Empirical evidence highlighted the innervation of bone tissue by nerve fibers, involving bone marrow and periosteum, as well as their fundamental role in fracture healing through infiltration into the callus during repair [9]. Among neurotrophic factors, nerve growth factor (NGF), the earliest discovered, has been extensively characterized for its involvement in neuronal regeneration and repair. Notably, recent investigations have uncovered a multifaceted function of NGF in osteogenesis, where it facilitates the extension of nerve fibers into nascent bone and callus and augments the vascular microenvironment [6].

In the specialized context of oral and maxillofacial surgery, NGF has been implicated in critical reparative processes, comprising mandibular defect reconstruction, peri-implant osteointegration, and tooth mineralization [10]. Nonetheless, the underlying mechanisms through which NGF modulates osteogenesis, whether by mediating nerve fiber innervation of bone tissue or by directly activating osteogenic cells and regulatory peptides, remain to be wholly elucidated. Given the synergistic osteogenic potential of BMP9 and NGF, a deeper exploration of their combined impact on the osteogenic differentiation of MSCs is essential for advancing regenerative strategies [8].

In the present investigation, it was attempted to elucidate the synergistic link of BMP9 with NGF in modulating the osteogenic differentiation of C3H10T1/2 MSCs. Through a comprehensive evaluation of the expression dynamics of critical osteogenic markers and the quantification of calcified nodule formation, the outcomes supported comprehending of the molecular and cellular mechanisms uncovering the combined effects of BMP9 and NGF. By integrating these findings into the broader framework of bone tissue engineering and regenerative medicine, a foundational paradigm could be established to optimize osteogenic therapeutics.

## Materials and methods

### Cell culture and maintenance of C3H10T1/2 and 293T cells

The murine mesenchymal stem cell line C3H10T1/2 (CCL-226TM, ATCC, USA) was selected for all experimental efforts, serving as a robust model for osteogenic differentiation studies. Cells were propagated in 250 mL culture flasks involving high-glucose Dulbecco's modified Eagle's medium (H-DMEM) acquired from Hyclone, headquartering in USA, which enriched with 10% fetal bovine serum (FBS; Gibco) headquartering in USA, 100 U/mL penicillin, and 100 μg/mL streptomycin. It was attempted to precisely maintain cultures at 37 °C particularly in a humidified atmosphere involving 5% $CO_2$ to ensure optimal growth conditions. Subculturing was undertaken at intervals of 36 to 48 h once cellular confluence reached approximately 70–80%, with experimental consistency being upheld by restricting the use of cells to passages 4–6. Notably, 293T cells, attained from the Key Biological Laboratory of the Affiliated Stomatological Hospital of Chongqing Medical University, were utilized for the amplification of recombinant adenoviruses. It was attempted to cultivate them in 100 mm Petri dishes with

DMEM acquired from Hyclone, supplemented with 10% FBS, 100 U/mL penicillin, and 100 μg/mL streptomycin. Cultivation conditions, involving temperature, humidity, and $CO_2$ levels, were precisely aligned with those of the C3H10T1/2 cells to ensure uniformity. Passaging of 293T cells was conducted when confluence approached 70–80%.

#### Recombinant adenovirus amplification and transfection

Recombinant adenoviruses encoding BMP9 (Ad-BMP9) and GFP (Ad-GFP) were generously provided by Professor Tongchuan He from the Laboratory of Medical Molecular Oncology, University of Chicago. To propagate these viral constructs, seeding of 293T cells into 100 mm culture dishes was undertaken, which allowed to adhere over an 8-hour period. Subsequently, Ad-BMP9 or Ad-GFP was introduced at an optimal multiplicity of infection, calibrated according to the growth status and confluence of the cells. The infection was monitored until approximately 50% of the cells displayed morphological alterations, such as rounding and detachment, indicative of advanced viral replication. The infected cell suspension was collected and subjected to low-speed 5-minute centrifugation particularly at 1,000 rpm to concentrate the cells. The resulting cell pellet underwent a series of three freeze-thaw cycles, alternating between −80 °C and 37 °C, to achieve efficient viral particle release. The lysate containing recombinant adenoviruses was carefully clarified, aliquoted to prevent repeated freeze-thaw cycles, and stored at -20 °C for future utilization. For transduction experiments, seeding of C3H10T1/2 cells into 24-well culture plates was undertaken at a density of $3 \times 10^4$ cells/mL, which allowed to adhere firmly to the substrate. To amplify transduction efficiency, 4 μL of polybrene acquired from Sigma headquartering USA was added to each well prior to viral application. Subsequently, Ad-BMP9 or Ad-GFP was introduced to the cultures. Transduction efficiency was precisely tracked by assessing GFP fluorescence under a fluorescence microscope at predefined time intervals, 12-hour, 24-hour, 48-hour, 3-day, and 7-day post-transduction.

#### Experimental grouping and osteogenic induction

To elucidate the influences of NGF on osteogenic differentiation, C3H10T1/2 cells were subjected to a fully randomized experimental framework and stratified into four distinct groups:

1. **Control Group (N0)**: Cells cultivated in standard conditions devoid of β-NGF, serving as the negative control benchmark.
2. **N10 Group**: Cells exposed to β-NGF at a terminal concentration of 10 ng/mL.
3. **N50 Group**: Cells treated with β-NGF at a terminal concentration of 50 ng/mL.
4. **N100 Group**: Cells administered β-NGF at a terminal concentration of 100 ng/mL.

In each group, osteogenic differentiation was initiated using DMEM augmented with osteoinductive supplements: 10 mmol/L β-sodium glycerophosphate, 50 μg/mL vitamin C, and $1 \times 10^{-8}$ mol/L dexamethasone, which acquired from Solaibao Technology Co., Ltd., headquartering in China.

To further find out the combinatorial influences of bone morphogenetic protein 9 (BMP9) and NGF on osteogenesis, C3H10T1/2 cells were allocated into the following experimental groups:

1. **GFP Group**: Cells transfected with Ad-GFP to establish a baseline control, providing a null framework for subsequent comparisons.
2. **NGF Group**: Cells treated with β-NGF (R&D Systems, USA) to reveal the isolated osteogenic efficacy of NGF.
3. **BMP9 Group**: Cells transfected with Ad-BMP9 to figure out BMP9's role as a singular osteogenic stimulator.
4. **NGF + BMP9 Group**: Cells co-treated with β-NGF and Ad-BMP9 to find out the hypothesized synergistic link among these osteoinductive agents.

For all experimental groups, osteogenic differentiation was induced utilizing a standardized DMEM formulation enriched with the aforementioned osteoinductive agents.

#### RNA and protein extraction and expression analysis

It was attempted to isolate total RNA from C3H10T1/2 cells at 3-hour, 12-hour, and 9-day post-induction utilizing TRIzol® reagent acquired from Invitrogen headquartering in the USA in strict adherence to the manufacturer's protocol. Indication of concentration and purity of the extracted RNA was implemented spectrophotometrically by assessing absorbance particularly at 260 and 280 nm, with A260/A280 ratios exceeding 1.9 indicative of acceptable purity. Synthesis of cDNA was undertaken through the PrimeScript™ RT Reagent kit acquired from Takara headquartering in Japan, and the expression levels of BMP9, Runx2, Col I, and OPN were quantified via real-time PCR employing SYBR® Premix Ex Taq™ (Takara). As the endogenous reference gene, GAPDH was utilized for normalizing expression level across samples.

Extraction of proteins from C3H10T1/2 cells was implemented at 24-hour, 48-hour, and 12-day post-induction through the usage of RIPA lysis buffer (Biosharp, China), which enriched with PMSF (Biyuntian

Biotechnology Co., Ltd., China) as a protease inhibitor to preserve protein integrity. It was attempted to quantify protein concentrations through the BCA Protein Concentration Assay kit acquired from Biyuntian Biotechnology Co., Ltd. Equivalent protein amounts were resolved via SDS-PAGE, followed by their transferring onto PVDF membranes (Biyuntian Biotechnology Co., Ltd.). The blockage of membranes was implemented utilizing 5% BSA particularly for 2-hour at ambient temperature, followed by overnight incubation at 4 °C with primary antibodies specific to Runx2, Col I, and OPN (Immunoway, USA), as well as GAPDH acquired from Bioworld headquartering in USA. Post-washing, the membranes' incubation was undertaken utilizing HRP-conjugated secondary antibodies (Bioworld), and immunodetection was implemented via an ECL Chemiluminescence kit (Biyuntian Biotechnology Co., Ltd.) on the ChemiDoc™ Imaging system acquired from Bio-Rad headquartering in USA.

#### ALP staining and quantification

To figure out alkaline phosphatase (ALP) activity, C3H10T1/2 cells were subjected to osteogenic differentiation for a duration of 7-day. Thereafter, immobilization of the cells was undertaken utilizing 4% paraformaldehyde acquired from Solaibao Technology Co., Ltd., headquartering in China, for 30-minute at ambient temperature. Post-fixation, it was attempted to perform ALP staining employing an ALP Staining kit acquired from Sangon Bioengineering Co., Ltd., headquartering in China, on the basis of the manufacturer's protocol. The examination of staining intensity was implemented under a light microscope, and micrographs were acquired to facilitate comparative analysis across distinct treatment groups. Quantitative assay of ALP activity entailed lysing the differentiated C3H10T1/2 cells in 0.1% Triton X-100 at two temporal endpoints, specifically 3- and 7-day post-osteogenic induction. The resultant lysates were incubated with an ALP-specific substrate, and enzymatic activity's evaluation was through measuring absorbance especially at 405 nm with the assistance of a microplate analyzer acquired from PerkinElmer (USA).

To evaluate the degree of extracellular matrix mineralization, Alizarin Red S staining was undertaken on C3H10T1/2 cells following 14- and 21-day of osteogenic differentiation. The 0.2% Alizarin Red S solution was prepared and adjusted to a pH of 4.2 using ammonium hydroxide to optimize calcium binding during staining. The cells were 30-minute fixed with 4% paraformaldehyde, thoroughly rinsed with PBS, and subsequently underwent incubation with a 0.2% Alizarin Red S solution attained from Solaibao Technology Co., Ltd. at 37 °C for a duration ranging from 40-minute to 2-hour. Excessive staining solution was meticulously removed by repeated rinsing with ultrapure water, and calcified nodules' visualization was implemented through microscopic imaging.

To quantitatively assess calcium deposition, a calcium content assay was performed at the 21-day osteogenic induction time point using the Calcium Assay Kit (Beyotime, China) following the manufacturer's protocol. Briefly, C3H10T1/2 cells were lysed in 0.5 M HCl and incubated at room temperature for 24 h to extract calcium ions. The calcium concentration in the supernatant was then quantified via a colorimetric reaction with o-cresolphthalein complexone at 575 nm using a microplate reader (SpectraMax iD3; Molecular Devices, San Jose, CA, USA). The results were normalized to total protein content, which was determined using a BCA Protein Assay Kit (Beyotime), to ensure accurate comparisons across experimental groups.

#### Statistical analysis

It was attempted to undertake experimental procedures particularly in triplicate, and the expression of resulting data was in the format of mean plus/minus the standard deviation (SD). Implementing statistical analysis was through SPSS software, wherein intergroup differences' evaluation was carried out through one-way analysis of variance (ANOVA). This was subsequently followed by Tukey's post-hoc test to facilitate pairwise comparisons particularly among multiple groups. Representation of statistical significance was linked to a threshold P-value falling below 0.05.

## Results

### Early osteogenic differentiation: Runx2 and OPN expression

#### *Runx2 and OPN mRNA expression levels*

To delineate the regulatory influences of NGF on the initiation of osteogenic differentiation, the transcriptional level of Runx2 mRNA was quantified in C3H10T1/2 cells following 3-day osteogenic induction through RT-PCR. The analysis unveiled a remarkable augmentation of Runx2 mRNA expression in experimentally fundamental groups subjected to NGF at concentrations of 10, 50, and 100 ng/ml relative to the untreated control group (n0) ($P < 0.001$). Noteworthy, the 10 ng/ml NGF group exhibited the apex of Runx2 mRNA expression, surpassing the levels identified in the higher concentration groups ($P < 0.01$ or $P < 0.001$) (Fig. 1).

Moreover, to characterize markers indicative of advanced osteogenic differentiation, evaluation of the expression levels of OPN mRNA was implemented following 9-day differentiation. RT-PCR outcomes uncovered remarkably escalated OPN mRNA expression in the NGF, BMP9, and NGF + BMP9 treatment groups relative to the control ($P < 0.05$, $P < 0.01$, or $P < 0.001$). Notably, the

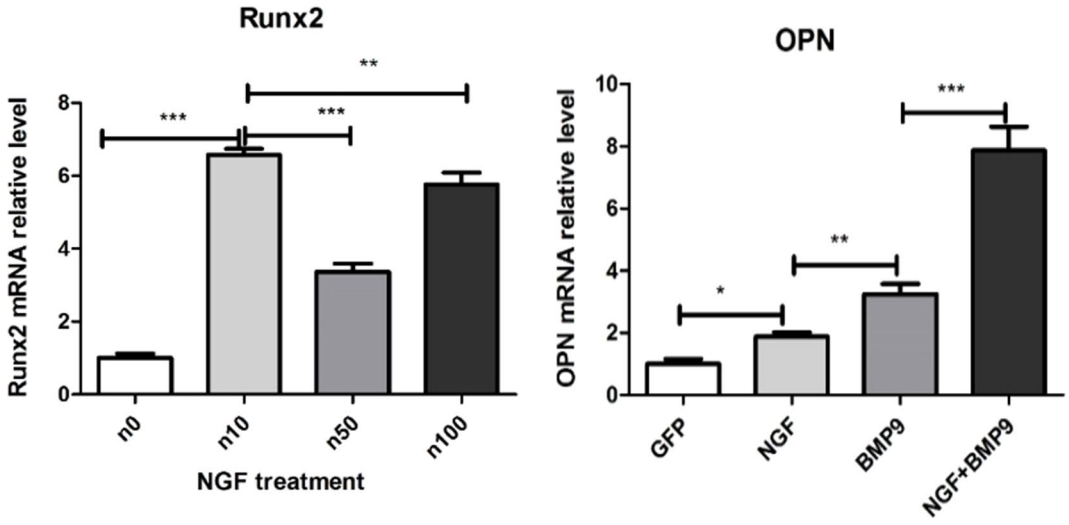


**Fig. 1** Evaluating Runx2 mRNA expression in C3H10T1/2 cells at 3-day post-induction of osteogenic differentiation, and indication of statistical significance was through single, double, and triple asterisks for P-thresholds below 0.05, 0.01, and 0.001, respectively. Concurrently, OPN mRNA expression level was assayed across all experimental groups following 9-day osteogenic differentiation, and indication of statistical significance was through single, double, and triple asterisks for P-thresholds below 0.05, 0.01, and 0.001, respectively. Scale bar: 100 μm

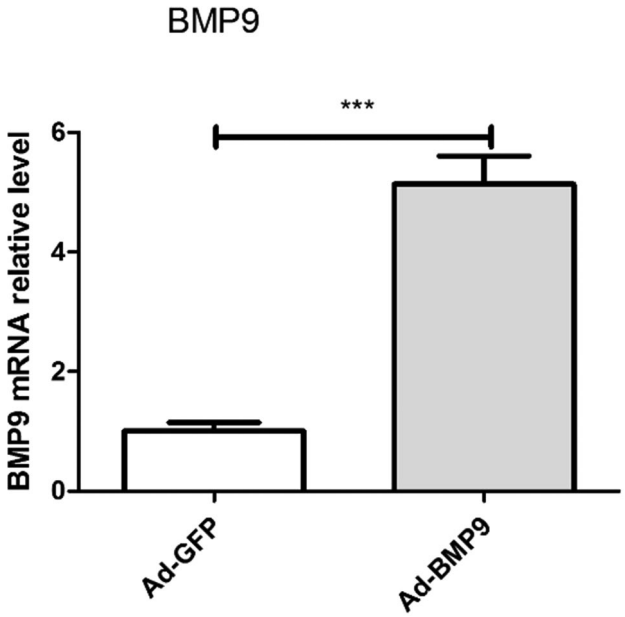


**Fig. 2** BMP9 mRNA expression level in C3H10T1/2 cells following 12-hour transfection with Ad-BMP9. Note: Indication of statistical significance was through single, double, and triple asterisks for P-thresholds below 0.05, 0.01, and 0.001, respectively. Scale bar: 50 μm

NGF + BMP9 combinatory treatment elicited the most robust upregulation of OPN mRNA expression, reflecting a synergistic link among these factors in promoting late-stage osteogenic marker expression ($P < 0.001$) (Fig. 1).

To further substantiate the transfection efficiency, quantification of *BMP9*'s mRNA expression level was undertaken through RT-PCR. The findings unveiled a remarkable escalation of *BMP9* mRNA in the Ad-BMP9 group, with a remarkable 5.14-fold elevation identified

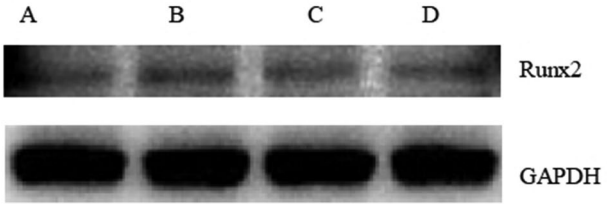


**Fig. 3** Runx2 protein expression level in C3H10T1/2 cells following 3-day osteogenic differentiation. **A**: n0 group; **B**: n10 group; **C**: n50 group; **D**: n100 group. Scale bar: 50 μm

12-hour post-transfection in contrast to the control group. This outcome reflects the successful transfection and escalated expression of *BMP9* in the treated cells ($P < 0.001$) (Fig. 2).

#### *Runx2 and OPN protein expression*

It was attempted to quantify the protein expression of Runx2 following 3-day osteogenic differentiation in C3H10T1/2 cells through Western blotting (WB). The findings uncovered the presence of Runx2 protein in both fundamental experimental/control groups. Notably, among the NGF-treated groups, the 10 ng/ml NGF group (n10) exhibited the most remarkable expression of Runx2, as evidenced by the enhanced intensity of the protein bands, highlighting a noticeable escalation of Runx2 protein level in the mentioned group (Fig. 3). Although band intensity differences were visually evident in Fig. 3, WB quantification was not included in this figure as the primary concentration was on confirming the presence and relative expression trends of Runx2 protein. However, similar WB quantification was conducted in Fig. 4 to substantiate these findings at additional time points.

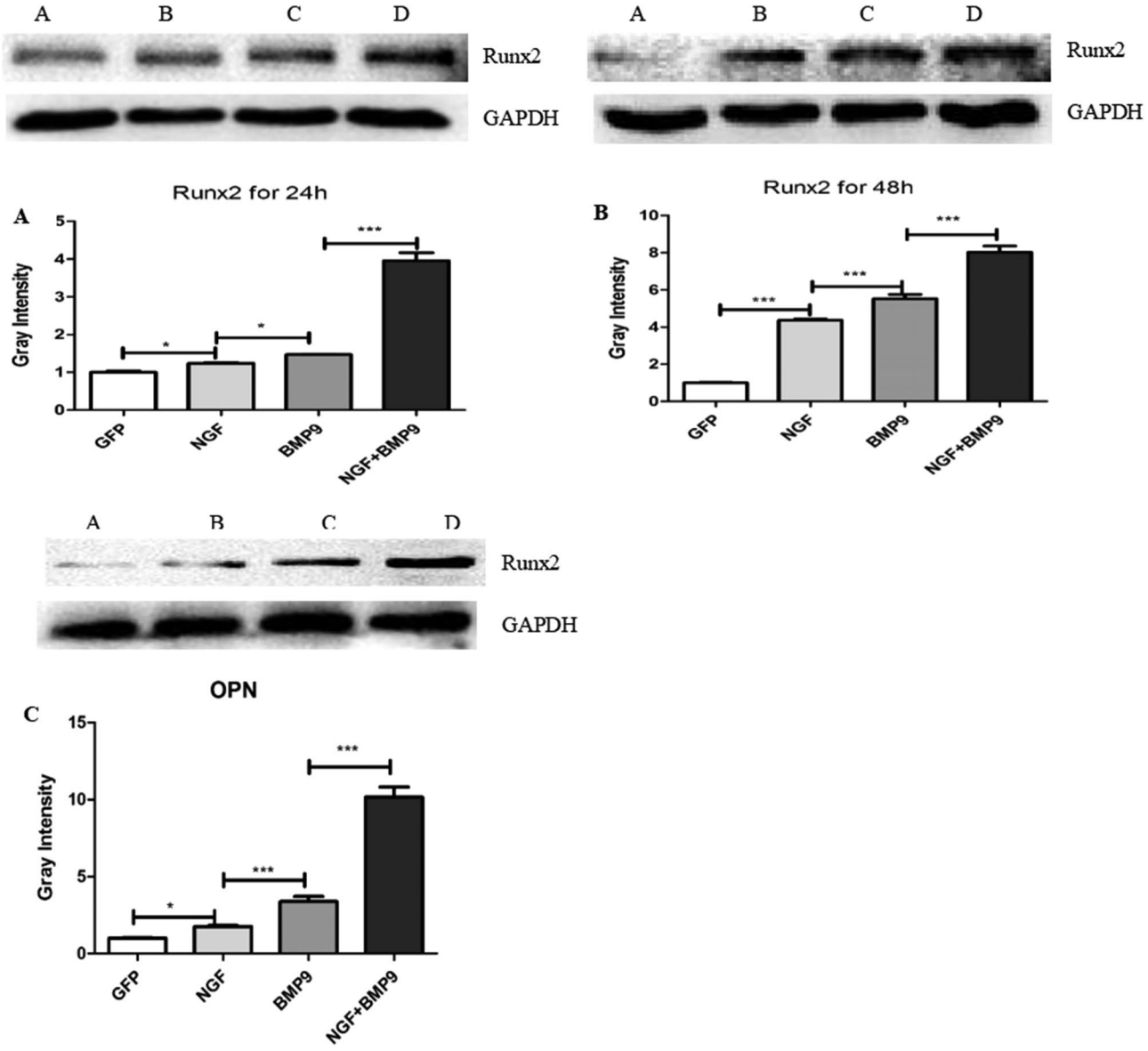


**Fig. 4** **A** and **B.** Runx2 protein expression level in each group following 24-hour C3H10T1/2 osteogenic differentiation. **A**: GFP group; **B**: NGF group; **C**: BMP9 group; **D**: NGF + BMP9 group. **E**: For gray value, indication of statistical significance was through single, double, and triple asterisks for P-thresholds below 0.05, 0.01, and 0.001, respectively. Following 48-hour C3H10T1/2 bone differentiation, **F**: GFP group; **G**: NGF group; **H**: BMP9 group; **I**: NGF + BMP9 group. **J**: For gray value, indication of statistical significance was through single, double, and triple asterisks for P-thresholds below 0.05, 0.01, and 0.001, respectively. and (**C**), OPN protein expression level in C3H10T1/2 cells following 12-day osteogenic differentiation. **A**: GFP group; **B**: NGF group; **C**: BMP9 group; **D**: NGF + BMP9 group. **E**: Gray value. Note: Indication of statistical significance was through single, double, and triple asterisks for P-thresholds below 0.05, 0.01, and 0.001, respectively. Scale bar: 100 μm

Additionally, WB coupled with subsequent gray value quantification demonstrated a noticeable upregulation of *Runx2* protein expression in the NGF, BMP9, and NGF + BMP9 treatment groups relative to the control group following 24-hour osteogenic differentiation ($P < 0.05$ or $P < 0.001$). Of which, the NGF + BMP9 group exhibited the most notable expression of *Runx2*, as indicated by the highest intensity of protein bands ($P < 0.001$). This pattern was consistently identified after 48-hour, with the NGF + BMP9 group maintaining the greatest *Runx2* protein expression ($P < 0.001$) (Fig. 4A and B).

In contrast, WB of OPN protein level after 12-day differentiation unveiled remarkably elevated OPN expression across all experimental groups relative to the control ($P < 0.05$ or $P < 0.001$). Remarkably, the NGF + BMP9 group exhibited the most noticeable OPN expression, reflecting the synergistic interaction of NGF with BMP9 on late-stage osteogenic differentiation ($P < 0.001$) (Fig. 4C).


**Fig. 5** ALP staining in C3H10T1/2 cells following 7-day osteogenic differentiation (×40 magnification). **A**: n0 group; **B**: n10 group; **C**: n50 group; **D**: n100 group. Scale bar: 200 μm

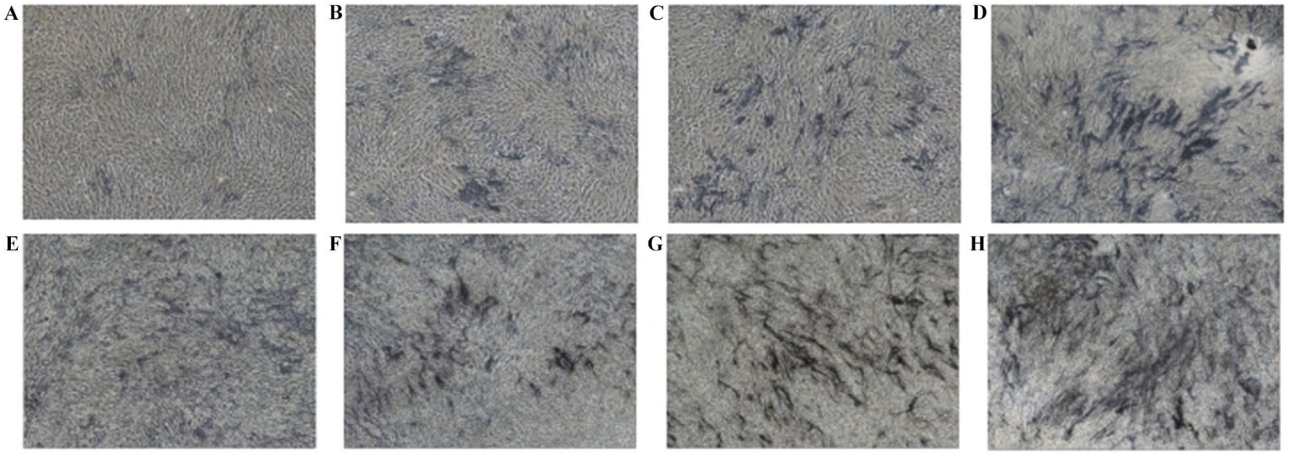


**Fig. 6** ALP staining in C3H10T1/2 cells in each group following 3- and 7-day osteogenic differentiation (×40 magnification). **A**: GFP group; **B**: NGF group; **C**: BMP9 group; **D**: NGF + BMP9 group (3d). **E**: GFP group; **F**: NGF group; **G**: BMP9 group; **H**: NGF + BMP9 group (7d). Scale bar: 200 μm

## ALP activity and staining

### *ALP staining and activity quantification*

ALP activity, a notable indicator of early osteogenic differentiation, was figured out through ALP staining following 7-day osteogenic induction. The findings uncovered distinct blue-stained areas, signifying the presence of ALP activity, in both fundamental experimental/control groups. However, the intensity and extent of the staining were most remarkable in the group treated with 10 ng/ml NGF, reflecting a substantial enhancement of ALP activity. This outcome demonstrates that the 10 ng/ml NGF treatment facilitated a more robust osteogenic differentiation, as evidenced by the elevated ALP activity at this concentration (Fig. 5).

Furthermore, ALP staining was implemented to visually find out osteogenic differentiation's progression in C3H10T1/2 cells. At both 3- and 7-day differentiation, the presence of blue or blue-black staining, suggestive of ALP activity, was noticeable in all groups. The NGF + BMP9 group exhibited the most remarkable and extensive staining, reflecting a more advanced degree of osteogenic differentiation. The staining intensity and distribution expanded over time, with the NGF + BMP9 group exhibiting the most substantial alterations (Fig. 6).

ALP activity, a well-described marker of early osteogenic differentiation, was quantitatively figured out at 3- and 7-day post-induction. The findings uncovered that ALP activity was noticeably elevated in the NGF, BMP9, and NGF + BMP9 treatment groups relative to the control group following 3-day differentiation ($P < 0.001$). Notably, the NGF + BMP9 group exhibited the most remarkable upregulation of ALP activity. This pattern was sustained following 7-day, with the NGF + BMP9 group consistently demonstrating the greatest ALP activity across all experimental groups ($P < 0.001$) (Fig. 7).

## Calcium nodule formation and advanced osteogenic markers

### *Alizarin red staining for calcium nodule formation*

To evaluate the effects of NGF on late-stage osteogenic differentiation, Alizarin Red S staining was performed to assess calcium nodule formation after 21 days. Red-stained calcium nodules were observed in all experimental and control groups. The 10 ng/ml NGF group exhibited the highest nodule count, suggesting enhanced mineralization (Fig. 8). Alizarin Red staining at 14 and 21 days revealed that all experimental groups exhibited calcium nodules, with the NGF + BMP9 group displaying

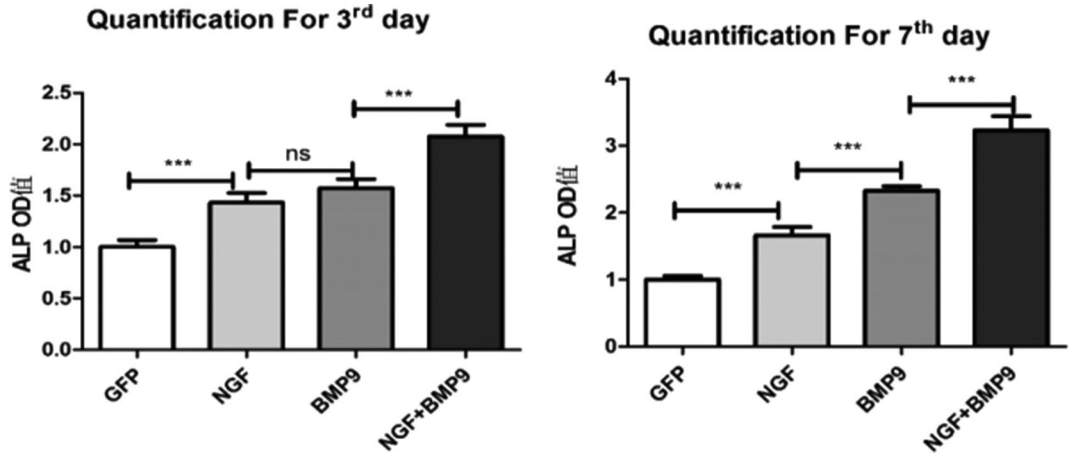


**Fig. 7** ALP activity level in C3H10T1/2 cells in each group following 3- and 7-day osteogenic differentiation. Note: Indication of statistical significance was through single, double, and triple asterisks for P-thresholds below 0.05, 0.01, and 0.001, respectively. Scale bar: 100 μm

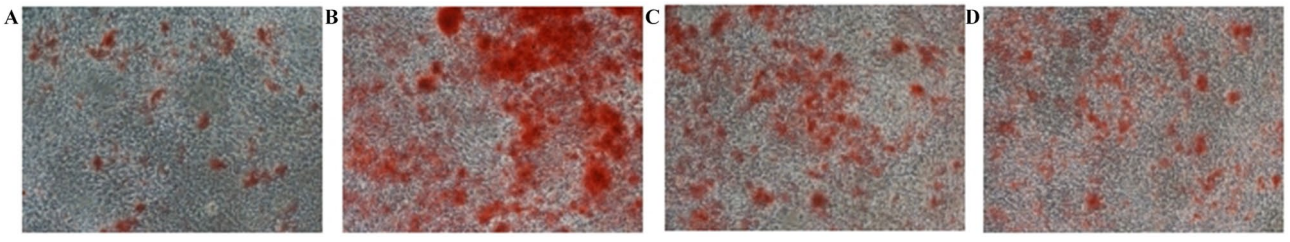


**Fig. 8** Calcium nodule formation in C3H10T1/2 cells following 21-day osteogenic differentiation (×40 magnification). **A**: n0 group; **B**: n10 group; **C**: n50 group; **D**: n100 group. Scale bar: 200 μm

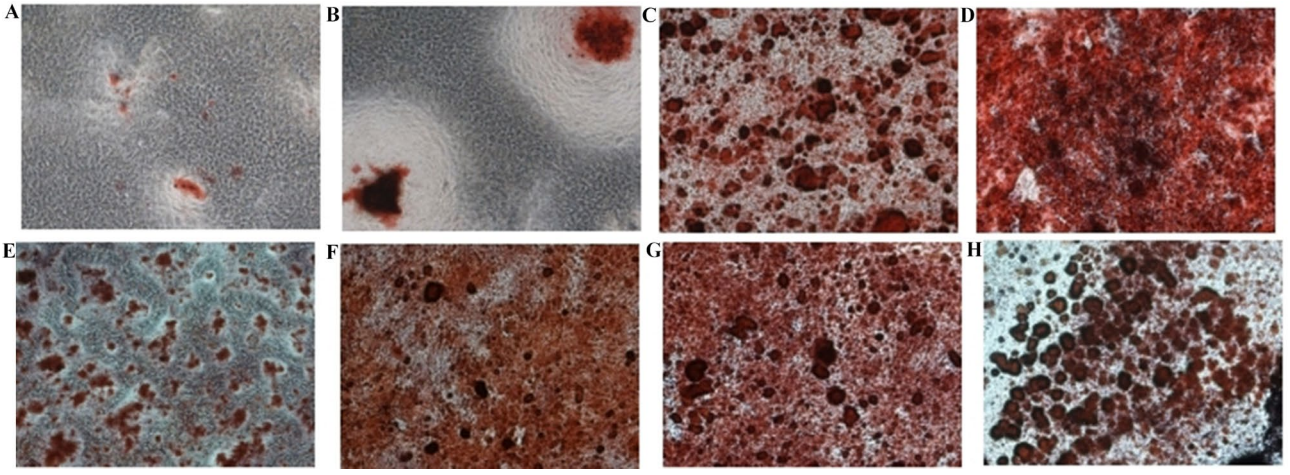


**Fig. 9** Calcium nodule formation in C3H10T1/2 cells in each group after 14- and 21-day osteogenic differentiation (×40 magnification). **A**: GFP group; **B**: NGF group; **C**: BMP9 group; **D**: NGF + BMP9 group (14d). **E**: GFP group; **F**: NGF group; **G**: BMP9 group; **H**: NGF + BMP9 group (21d). Scale bar: 200 μm

the most extensive nodule formation. The number of nodules significantly increased over time, particularly in the NGF + BMP9 group, highlighting its role in promoting osteogenic mineralization (Fig. 9).

Quantitative analysis of calcium deposition further confirmed the enhanced mineralization observed in Alizarin Red S staining. The calcium content assay revealed significantly higher calcium levels in the NGF, BMP9, and NGF + BMP9 treatment groups compared to the control group ($P < 0.05$, $P < 0.01$, or $P < 0.001$, respectively). Notably, the NGF + BMP9 group exhibited the highest calcium deposition, with an approximately 2-fold increase over the control group, further supporting the synergistic effect of these osteoinductive factors on late-stage osteogenic differentiation.

#### *Microscopic morphology and effects of Ad-BMP9 transfection*

The efficiency of Ad-BMP9 transfection in C3H10T1/2 cells was evaluated via fluorescence microscopy. Cells were infected with Ad-BMP9 and Ad-GFP at an optimal viral concentration of 4 μl/ml, achieving an infection efficiency of approximately 30%. Green fluorescence was detected in transfected cells after 12 h, confirming successful Ad-BMP9 expression (Fig. 10).

#### *Runx2 and col I mRNA expression*

To assess the impact of BMP9 and NGF on early osteogenic differentiation, Runx2 and Col I mRNA expression levels were quantified via RT-PCR. After 3 h of induction, Runx2 and Col I mRNA levels were significantly upregulated in NGF, BMP9, and NGF + BMP9 groups compared to the control ($P < 0.05$, $P < 0.01$, or $P < 0.001$). The NGF + BMP9 group exhibited the highest expression levels ($P < 0.001$). This trend persisted after 12 h, confirming the synergistic enhancement of early osteogenic markers by NGF and BMP9 ($P < 0.001$) (Fig. 11).

## Discussion

This investigation provided substantial evidence supporting the role of NGF in modulating osteogenic differentiation in C3H10T1/2 MSCs, particularly in upregulating key osteogenic markers, including Runx2 and OPN. The significant increase in Runx2 mRNA expression in NGF-treated groups, especially at the 10 ng/ml concentration, highlights NGF's potency in the early stages of osteogenic differentiation. This finding aligns with previous studies indicating that Runx2 is a pivotal transcription factor essential for osteoblast differentiation, as it regulates the activation of osteogenic genes and subsequent bone formation [9]. The dose-dependent response, in which the highest expression was observed at 10 ng/ml, suggests an optimal NGF concentration, beyond which additional increases do not proportionally enhance osteogenic differentiation, in accordance with known growth factor signaling mechanisms [10].

A critical observation is the significant upregulation of OPN mRNA levels in the NGF, BMP9, and NGF + BMP9 groups, underscoring the role of these factors in promoting osteogenesis. OPN, a late-stage marker of osteoblast differentiation and mineralization, is crucial for matrix stabilization and bone remodeling [11]. The highest OPN expression in the NGF + BMP9 group suggests a synergistic interaction, wherein NGF and BMP9 jointly enhance osteogenic potential more effectively than either factor alone. This synergy likely arises from crosstalk between NGF-activated TrkA receptor signaling and the BMP9-mediated Smad-dependent pathway, as well as non-canonical pathways such as MAPK signaling [12]. The convergence of these signaling cascades may amplify transcriptional activation of osteogenic genes, facilitating robust differentiation. This interaction is consistent with previous reports demonstrating that growth factors can exert combinatorial effects by modulating parallel and intersecting intracellular pathways [11].

The effective transfection of C3H10T1/2 cells with Ad-BMP9, confirmed by the significant elevation in BMP9 mRNA expression, validates the efficiency of the adenoviral vector in gene delivery. This finding, coupled with the enhanced osteogenic differentiation observed, aligns with BMP9's well-documented role in promoting osteoblast differentiation and bone formation [13]. The synergy observed with NGF is likely attributed to BMP9's potent osteoinductive capacity, which complements NGF-induced signaling events, particularly via

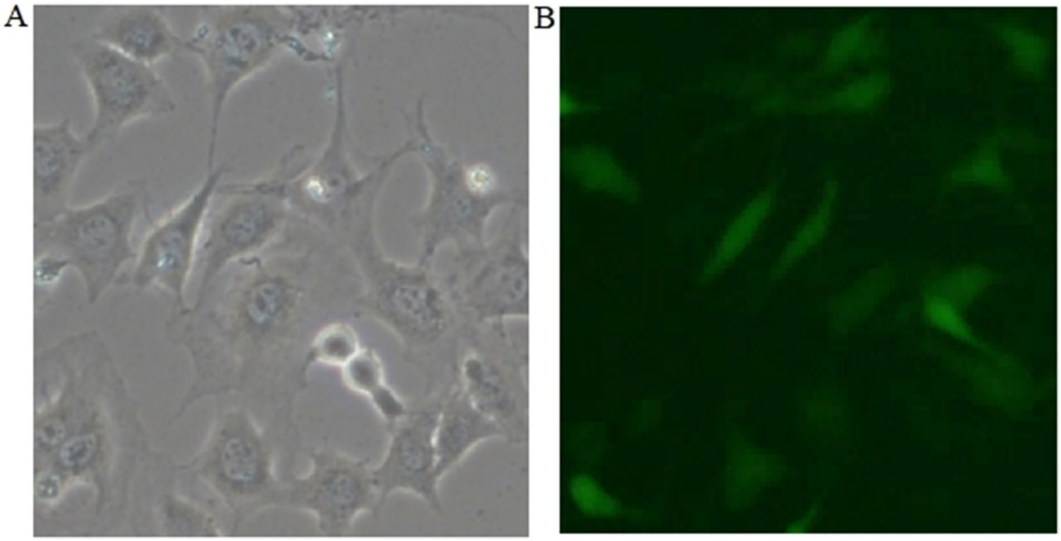


**Fig. 10** Microscopic morphology of C3H10T1/2 cells following 12-hour transfection with Ad-BMP9 (×100 magnification). **A**: C3H10T1/2 under an inverted microscope; **B**: C3H10T1/2 under a fluorescence microscope. Scale bar: 50 μm

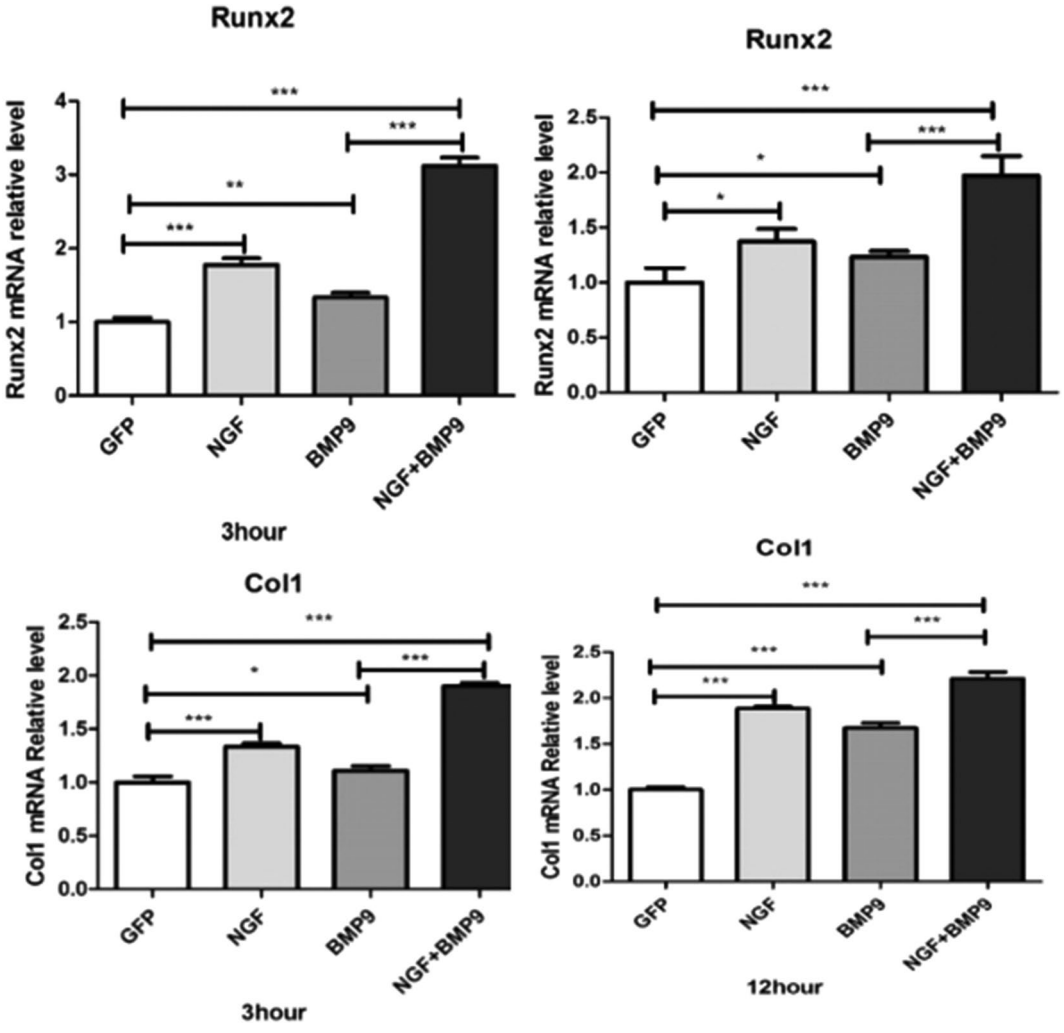


**Fig. 11** mRNA expression levels of Runx2 and Col I in each group following 3- and 12-hour C3H10T1/2 osteogenic differentiation. Note: Indication of statistical significance was through single, double, and triple asterisks for P-thresholds below 0.05, 0.01, and 0.001, respectively. Scale bar: 100 μm

the activation of Smad1/5/8 and MAPK pathways. Previous research has demonstrated that BMP9 can strongly induce Runx2 expression through Smad-dependent mechanisms, while NGF-mediated signaling enhances Runx2 activity through ERK and PI3K/Akt pathways [14]. The convergence of these pathways may explain the pronounced upregulation of Runx2 and OPN observed in the NGF + BMP9 group.

WB further corroborate these findings, revealing that Runx2 protein levels were significantly elevated in NGF, BMP9, and NGF + BMP9 groups, with the NGF + BMP9 group displaying the most robust expression. Runx2 serves as a master regulator of osteoblast differentiation by initiating the transcription of downstream osteogenic genes, including OPN and Col I, thereby contributing to the maturation of osteoblasts and extracellular matrix deposition [15]. The sustained elevation of Runx2 and OPN protein levels after 12-day differentiation reinforces the idea that NGF and BMP9 co-regulate osteogenesis at both transcriptional and translational levels. These results are consistent with prior studies demonstrating that the integration of multiple growth factors can enhance osteogenesis more effectively than single-factor treatments [16].

The assessment of ALP activity, an early osteogenic differentiation marker, provides additional insights into the functional implications of NGF and BMP9 co-stimulation. The remarkable ALP staining in the 10 ng/ml NGF group after 7-day differentiation suggests that this concentration is particularly effective in promoting early osteogenesis. The most intense and widespread ALP staining in the NGF + BMP9 group correlates with increased Runx2 and OPN expression, suggesting a robust osteogenic response induced by the combined treatment. This observation is consistent with the concept of growth factor synergy, wherein NGF and BMP9 may cooperatively enhance osteoblast differentiation

through the activation of overlapping intracellular signaling pathways [17].

The formation of calcium nodules, as assessed by Alizarin Red S staining, further supports the synergistic role of NGF and BMP9 in late-stage osteogenic differentiation. The significantly higher number of calcium nodules in the NGF + BMP9 group after 21-day differentiation underscores the long-term effectiveness of this combined treatment in promoting mineralization. This effect is likely mediated by the cooperative activation of Runx2 and downstream matrix-associated proteins, which are critical for mineral deposition and bone matrix maturation. Previous studies have similarly reported enhanced osteogenic differentiation with combinatorial growth factor approaches, reinforcing the notion that integrating NGF and BMP9 can optimize osteoblast activity for applications in bone tissue engineering [17, 18].

The significant upregulation of Runx2 and Col I mRNA in response to BMP9 and NGF treatment provides further mechanistic insights into the regulation of early osteogenic differentiation. Runx2 is a key transcriptional regulator, while Col I serves as an essential structural component of the bone extracellular matrix, collectively contributing to bone tissue formation [19]. The early and sustained upregulation of these markers in the NGF + BMP9 group suggests that NGF may facilitate BMP9-driven osteogenesis by modulating Runx2 activity and extracellular matrix organization. This combinatorial approach could have significant implications for bone regeneration strategies, as it capitalizes on the molecular synergy between neurotrophic and osteogenic signaling pathways.

Overall, the findings suggest that NGF and BMP9 synergistically promote osteogenic differentiation through multiple converging mechanisms, including TrkA and Smad/MAPK crosstalk, enhanced Runx2 activation, and extracellular matrix remodeling. These insights provide a strong rationale for exploring NGF and BMP9 co-stimulation in bone tissue engineering applications, where optimized osteogenesis is crucial for effective bone regeneration.

## Conclusions

The present investigation elucidated the potent synergistic influences of BMP9 and NGF in fostering the osteogenic differentiation of C3H10T1/2. When administered in combination, BMP9 and NGF remarkably escalated essential osteogenic markers' levels, involving Runx2, Col I, and OPN, while also augmenting ALP activity and facilitating the formation of mineralized nodules. These outcomes highlight that the dual treatment of BMP9 and NGF could result in a more favorable microenvironment for osteogenesis, thereby expediting both the early and later stages of osteogenic differentiation. The enhanced osteogenic response triggered by this BMP9-NGF combination represents a promising direction for advancing bone tissue engineering plus regenerative medicine. Furthermore, this therapeutic scheme holds substantial potential for addressing bone defects, fractures, and other skeletal pathologies, providing a framework for developing novel protocols that capitalize on the synergistic link of BMP9 with NGF. To fully translate these in vitro outcomes into clinical practice, future research is essential to validate the findings in vivo, investigate the underlying molecular mechanisms governing the BMP9-NGF synergy, and refine dosing and delivery methods to optimize therapeutic outcomes. Consequently, the integration of BMP9 and NGF is noteworthy for advancing bone regeneration therapies, with the potential to substantially update patient outcomes in orthopedic and reconstructive medicine.

#### Abbreviations

| | |
|---|---|
| MSCs | Mesenchymal stem cells |
| BMPs | Bone morphogenetic proteins |
| GDF-2 | Growth differentiation factor 2 |
| TGF-β | Transforming growth factor-β |
| NGF | Nerve growth factor |

#### Acknowledgements

Not applicable.

#### Author contributions

Yinghui Tan: conceptualization, resources, supervision, and writing—review and editing; Kun Yang: methodology, software, investigation and formal analysis; Gang Li: methodology, software, investigation and formal analysis; Junyu Liu: visualization, investigation and writing—original draft; All authors contributed to the article and approved the submitted version.

#### Funding

This study was supported by the National Natural Science Foundation of China (81371110).

#### Data availability

The original achievements that underpin this investigation are comprehensively detailed in the main text and supplementary materials provided. For those requiring further elaboration or wishing to engage in deeper discourse, the corresponding author remains available for direct inquiry.

## Declarations

#### Ethics approval and consent to participate

Not applicable.

#### Consent for publication

Not applicable.

#### Competing interests

The authors declare no competing interests.

#### Author details

[1]Chongqing Key Laboratory of Oral Diseases, The Affiliated Stomatological Hospital of Chongqing Medical University, No.426 Songshi North Road, Yubei District, Chongqing 401147, China
[2]Department of Periodontology, Affiliated Stomatology Hospital of Zunyi Medical University, No.149 Dalian Road, Huichuan District, Zunyi City, Guizhou Province 563099, China

[3]Department of Stomatology, The First Affiliated Hospital of Army Medical University, No.29 Gaotanyan Main Street, Shapingba District, Chongqing 400038, China
[4]Department of Stomatology, The Second Affiliated Hospital of Army Medical University, No.83 Xinqiao Main Street, Shapingba District, Chongqing 400037, China

Received: 21 January 2025 / Accepted: 2 March 2025
Published online: 15 March 2025

**References**

1. Ferraz MP. Bone grafts in dental medicine: an overview of autografts, allografts and synthetic materials. Mater (Basel). 2023;16(11):4117.
2. Perez JR, Kouroupis D, Li DJ, Best TM, Kaplan L, Correa D. Tissue engineering and Cell-Based therapies for fractures and bone defects. Front Bioeng Biotechnol. 2018;6:105.
3. Xie Q, Wang Z, Zhou H, Yu Z, Huang Y, Sun H, et al. The role of miR-135-modified adipose-derived mesenchymal stem cells in bone regeneration. Biomater. 2016;75:279–94.
4. Andrés Sastre E, Nossin Y, Jansen, et al. A new semi-orthotopic bone defect model for cell and biomaterial testing in regenerative medicine. Biomater. 2021;279:121187.
5. Park JH, Koh EB, Seo YJ, Oh HS, Byun JH. BMP-9 improves the osteogenic differentiation ability over BMP-2 through p53 signaling in vitro in human Periosteum-Derived cells. Int J Mol Sci. 2023;24(20):15252.
6. Paz JERM, Adolpho LF, Ramos JIR, Bighetti-Trevisan RL, Calixto RD, Oliveira FS, et al. Effect of mesenchymal stem cells overexpressing BMP-9 primed with hypoxia on BMP targets, osteoblast differentiation and bone repair. Biology (Basel). 2023;12(8):1147.
7. Lian M, Qiao Z, Qiao S, Zhang X, Lin J, Xu R, et al. Nerve growth Factor-Preconditioned mesenchymal stem Cell-Derived Exosome-Functionalized 3D-Printed hierarchical porous scaffolds with Neuro-Promotive properties for enhancing innervated bone regeneration. ACS Nano. 2024;18(10):7504–20.
8. Ji Y, Mao Y, Lin H, Wang Y, Zhao P, Guo Y, et al. Acceleration of bone repairation by BMSCs overexpressing NGF combined with NSA and allograft bone scaffolds. Stem Cell Res Ther. 2024;15(1):194.
9. Chen Y, Zhao X, Wu H. Transcriptional programming in arteriosclerotic disease: A multifaceted function of the Runx2 (Runt-Related transcription factor 2). Arterioscler Thromb Vasc Biol. 2021;41(1):20–34.
10. Liu Z, Suh JS, Deng P, Bezouglaia O, Do M, Mirnia M, et al. Epigenetic regulation of NGF-Mediated osteogenic differentiation in human dental mesenchymal stem cells. Stem Cells. 2022;40(9):818–30.
11. Kusuyama J, Seong C, Nakamura T, Ohnishi T, Amir MS, Shima K, et al. BMP9 prevents induction of osteopontin in JNK-inactivated osteoblasts via Hey1-Id4 interaction. Int J Biochem Cell Biol. 2019;116:105614.
12. Li Q, Wu D, Li R, Zhu X, Cui S. Valproic acid protects neurons and promotes neuronal regeneration after brachial plexus avulsion. Neural Regen Res. 2013;8(30):2838–48.
13. Wang Y, Xia C, Chen Y, Jiang T, Hu Y, Gao Y. Resveratrol Synergistically Promotes BMP9-Induced Osteogenic Differentiation of Mesenchymal Stem Cells. Stem Cells Int. 2022;2022:8124085.
14. Li Y, Liu Z, Wang HD, Zhang J, Lin M, Yang J et al. HIF1α Promotes BMP9-Mediated Osteoblastic Differentiation and Vascularization by Interacting with CBFA1. Biomed Res Int. 2022;2022:2475169.
15. Yao X, Li P, Deng Y, Yang Y, Luo H, He B. Role of p53 in promoting BMP9induced osteogenic differentiation of mesenchymal stem cells through TGFβ1. Exp Ther Med. 2023;25(6):248.
16. Cui J, Zhang W, Huang E, Wang J, Liao J, Li R, et al. BMP9-induced osteoblastic differentiation requires functional Notch signaling in mesenchymal stem cells. Lab Invest. 2019;99(1):58–71.
17. Seong CH, Chiba N, Kusuyama J, Subhan Amir M, Eiraku N, Yamashita S, et al. Bone morphogenetic protein 9 (BMP9) directly induces Notch effector molecule Hes1 through the SMAD signaling pathway in osteoblasts. FEBS Lett. 2021;595(3):389–403.
18. Cheng C, Tang S, Cui S, Yang T, Li L, Zhai M, et al. Nerve growth factor promote osteogenic differentiation of dental pulp stem cells through MEK/ERK signalling pathways. J Cell Mol Med. 2024;28(4):e18143.
19. Lu X, Li L, Wu N, Chen W, Hong S, Xu M, et al. BMP9 functions as a negative regulator in the myogenic differentiation of primary mouse myoblasts. Biosci Biotechnol Biochem. 2023;87(11):1255–64.

## Publisher's note